Mem. S.A.It. Vol. 91, 346

Memorie della

Realistic simulations of relativistic jets

D. Mukherjee[1], G. Bodo[2], P. Rossi[2], and A. Mignone[3]

[1] Inter-University Centre for Astronomy and Astrophysics, Pune, India - 411007
e-mail: dipanjan@iucaa.in
[2] Istituto Nazionale di Astrofisica – Osservatorio Astrofisico di Torino, Via Osservatorio, 20, 10025 Pino Torinese, Italy
[3] Università degli Studi di Torino, Via Pietro Giuria 1, 10125 Torino, Italy

Abstract. We perform realistic 3D relativistic magnetohydrodynamic simulations of jets from super-massive blackholes. We employ the newly developed Lagrangian Particle module to simultaneously evolve spatial and spectral evolution of relativistic non-thermal electrons that produce synchrotron emission. Our simulations enable us to accurately predict the emission properties and the impact on observables due to variation in jet fluid and onset of jet instabilities.

1. Introduction

Supermassive blackholes in the centres of galaxies can launch powerful relativistic jets that grow to very large sizes, potentially affecting the evolution of the galaxy and its environment (Fabian 2012). Emission from relativistic jets is primarily dominated by synchrotron processes from relativistic electrons inside the jet and its cocoon (Worrall and Birkinshaw 2006). The synchrotron emission is dependent on both the strength and morphology of magnetic field distribution and the evolution of the non-thermal relativistic electron populations. In standard analytical theory of emission from jets(e.g. Pacholczyk 1970; Jaffe and Perola 1973), the evolution of the non-thermal electrons is often approximated with an average evolution of the electron spectra experiencing average magnetic fields in the cocoon. Such treatments cannot account for the local inhomogeneties in the magnetic field distribution expected to arise in turbulent jet cocoons due to MHD instabilities, as well as the time evolution of the fluid quantities. Additionally, the most important flaw of these methods is assuming a single shock structure, at the jet head, where the electrons are assumed to be accelerated. The accelerated spectra are often set without explicit input from realistic shock acceleration results. All of these assumptions render the modelling of the emission from relativistic jets to be dependent on highly uncertain approximate parameters.

Recent works (such as Mimica et al. 2004; Mimica and Aloy 2012; Turner and Shabala 2015) have resorted to semi-analytic modelling of the evolution of the electron spectra, embedding them in a fluid flow as a post-process step of a fluid simulation. These though indicative of results from a realistic system, do not self-consistently solve for the evolution of the electrons distribution, as the fluid parameters themselves change in a dynamic system. In a recent development (Vaidya et al. 2018), a new numerical module (the Lagrangian Particle module) has been implemented in the PLUTO MHD code that models the evolution of non-thermal electrons inside the simulation domain in real time (as opposed to post-process), duly accounting for the radiative energy losses as well as acceleration at shocks, following the principles of diffusive shock acceleration. We have utilised this novel approach to seed macroparticles within the jet, at every time step of the simulation, to represent the injection of non-thermal electrons by a jet. The macro-particles (which hereafter we refer to as Cosmic Ray Electrons or CREs) represent a collection of non-thermal electrons with a spectral distribution. We have carried out a suite of simulations with different jet properties, using this module, which for the first time enables us to study self-consistently study the spatial and spectral evolution of CREs in a realistic simulation of a relativistic jet from a super-massive blackhole.

2. Numerical setup

2.1. Fluid setup

We solve the equations of relativistic magnetohydrodynamics to simulate the evolution of a relativistic jet evolving into an ambient medium. The details of the simulation set up has been described in (Mukherjee et al. 2020), which we briefly summarise here. The jet is launched from an internal injection zone, within the domain of the simulation box. The jet pressure is set to be in equilibrium with the pressure of the ambient medium at the same height, except for simulation G, where the jet is over-pressured. The jet density is set to be fraction of the ambient density. The velocity and density contrast are set differently for different simulations to explore the dynamics and evolution for a varied range of jet powers. The jet is injected into an ambient medium that is kept in hydrostatic equilibrium with an external static gravitational field. A toroidal magnetic field is injected with the jet. The strength of the field is determined by considering the jet Poynting flux to be a fraction (jet magnetisation) of the relativistic enthalpy flux of the jet.

The simulations are performed with the PLUTO code (Mignone et al. 2007), using a HLLD Riemann solver (Mignone et al. 2009) to solve the relativistic magneto-hydrodyanamic equations. We employ a second order Runge-Kutta time stepping for the temporal evolution of the equations. The fluxes are reconstructed using a third order parabolic interpolation scheme (PPM as in Colella and Woodward 1984). The simulation is performed in a Cartesian coordinate system, in a computation domain of physical dimensions of $2.5 \times 2.5 \times 9$ kilo parsecs (kpc) for a typical simulation. The resolution of the simulation is set at 15 pc. The detailed list of the parameters for various simulations have been presented in Table 1 of Mukherjee et al. (2020).

2.2. Particle setup

The CRE macro-particles are injected in the simulation domain above the injection region of the jet, along the Z axis.Two CRE particles are injected in each computational cell cell for better spatial sampling of the jet cocoon. The CREs have an initially steep power-law spectrum ($\alpha_1 = 9$) and with Lorentz factors in the range $(\gamma_{\rm min}, \gamma_{\rm max}) \equiv (10^2, 10^6)$ as:

$$N(E) = n_m \left(\frac{1 - \alpha_1}{E_{\rm max}^{1-\alpha_1} - E_{\rm min}^{1-\alpha_1}} \right) E^{-\alpha_1} \qquad (1)$$

The injected CREs are accelerated at shocks to a new spectrum whose nature is given by the predictions of diffusive shock acceleration (DSA) theory, as outlined in detail in Vaidya et al. (2018). The spectrum of the pre-shock CRE is convolved with the DSA predicted power-law spectrum to get the final spectrum of a CRE as it exits a shock. The normalisation of the spectrum is set by enforcing CRE energy to be a fraction of the fluid internal energy (equipartition), which we take to be 0.1 for this work. The spectra of CREs not in a shock are duly updated to account for energy losses due to radiative processes such as synchrotron emission and inverse Compton interaction with CMB photons.

3. Results

As the CREs are advected with the jet flow, they are shocked within the jet at sites of recollimation shocks. This can be identified in

Table 1. List of simulations and parameters

Sim. label	Lorentz factor	Magnetisation	Jet power (in erg s^{-1})	No. Particles[a] ($\times 10^6$)
B[b]	3	0.1	2×10^{44}	16.4
D	5	0.01	1.1×10^{45}	6.5
E	5	0.05	1.2×10^{45}	18.0
F	5	0.1	1.2×10^{45}	3.2
G	6	0.2	8.3×10^{45}	14.9
H	10	0.2	1.6×10^{46}	9.8
J	10	0.1	1.5×10^{46}	55.3

[a] The total number of particles injected during the course of the simulation.
[b] The density contrast defined as the ratio of the jet density to ambient gas is 4×10^{-5}. For all other cases, the value is $\eta = 10^{-4}$

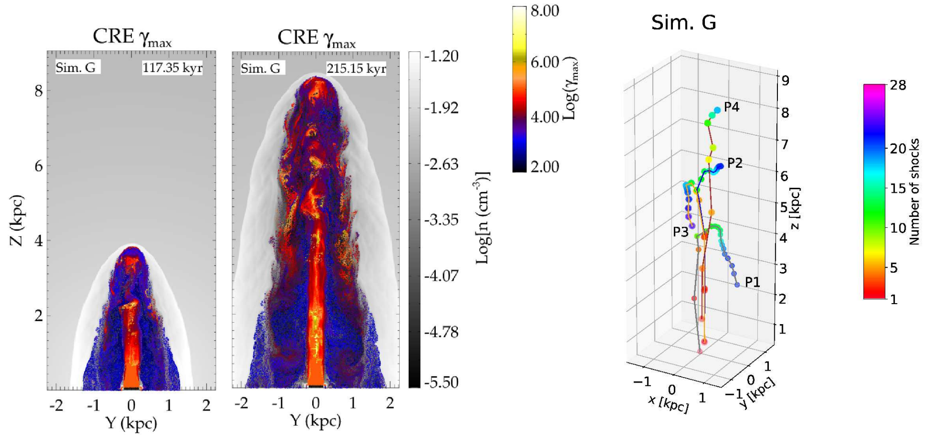

Fig. 1. Left and Middle: Density in the $Y - Z$ plane for simulation H. CREs with colors representing γ_{max}, the highest Lorentz factor of the CRE spectrum, are over-plotted on the density maps. The plot clearly shows newly accelerated CREs with high γ_{max} inside the jet, at regions where recollimation shocks converge. **Right:** Trajectories of 4 CREs that have undergone multiple shock encounters. The CREs are chosen to be ones that have undergone highest number of shock crossings at a given height.

Fig. 1, where the maximum Lorentz factor (γ_{max}) of each CRE in the $Y - Z$ plane has been over-plotted on the density map of the jet. Small islands of high γ_{max} within the jet spine are indicative of locations where CREs have recently exited a recolliamation shock. The jet spine is generally filled with freshly shocked energetic CREs. As the CREs cross the tip of the bow shock at the jet head, they are re-accelerated to high energies (denoted by the reddish patch near the jet-head).

Subsequently, the electrons stream down the backflow into the cocoon. This can be seen from the trajectories of some of the selected CREs, presented in the right panel of Fig. 1. The trajectories show the standard evolutionary picture of CREs, whereby they initially travel along the jet axis and undergo some acceleration due to recollimation shocks. They leave the jet axis after encountering the bow shock at the jet-head and flow back down along with the backflow in the cocoon. Some of the

CREs (P2 and P4) are shocked multiple times at the jet-head itself due to complex shock structures. Some CREs (P3 and P4) encounter further shocks inside the cocoon after exiting the jet, due to internal fluid turbulence in the cocoon.

The backflow is primarily filled with cooling electrons which have lost energy due to radiative losses, denoted by the bluish color of CRE particles in the jet cocoon in the left and middle panels of Fig. 1. However, at late times, weak internal shocks can occur inside the cocoon due to turbulent motions of the backflow in the jet cocoon. These internal shocks can further accelerate the CREs, as can be seen from the some energetic CREs in the jet cocoon, shown in the middle panel of Fig. 1.

We find that the evolution of the CRE spectrum strongly depend on the nature fluid instabilities that may be triggered as the jet evolves with different initial parameters. Strongly magnetised jets can develop kink instabilities that can create complex structures of the terminal shock. As CREs reach such a terminal shock and pass through them, they will be re-accelerated over an extended spatial scale. As the jet head moves over a wide solid angle due to the helical motions induced by the kink instabilities, shocked CREs are distributed over the jet cocoon. Such instabilities usually decelerate the jet, with the effect of filling the jet cocoon with highly energetic CREs that have been accelerated at the extended terminal shock.

Jets suffering from Kelvin Helmholtz instabilities on the other hand will create internal shocks inside the cocoon, instead of a complex terminal shock. CREs that travel back downwards with the backflow, are trapped inside the turbulent shock structures *inside the cocoon*, where they undergo multiple shock crossings. Thus CREs can be re-accelerated inside the cocoon, at sites of internal shocks (as shown in Fig. 1). This is well demonstrated in our simulations, which though conjectured, have not been demonstrated before. Such internal re-acceleration of the CREs have significant implications on the standard cooling models of electrons, which are widely used in the observational community to estimate the spectral ages of relativistic jets (Murgia et al. 1999).

The self-consistently evolved CRE spectra allow us to create maps of synchrotron surface brightness expected from such systems, as shown in Fig. 2. The emission at 1.4 Ghz, in the top panel of Fig. 2 shows the bright hostspot at the top, where the jet strongly interacts with the ambient medium, as is typical of Fanaroff-Riley II jets (Fanaroff and Riley 1974). The polarisation vectors show ordered, longitudinal orientation in the central regions, indicating a dominant toroidal magnetic field, due to the toroidal field injected at the jet flow inlet. The polarisation vectors in the cocoon are primarily laterally oriented, implying a longitudinal field in the backflow. This is expected, as the injected toroidal field is stretched to longitudinal structures in the backflow. The emission at 1.4 Ghz is more volume filling than the one in 15 GHz, with nearly homogeneous (on an average) emission in the cocoon, except for the jet head with the hotspot. At higher frequencies on the other hand, the jet axis is clearly discernible, as longitudinal structure from $\sim 0.2 - 4$ kpc. This is because the, cocoon hosts primarily older particles with lower maximum energy due to radiative losses. Hence they contribute minimally to emission at higher frequencies, except from the jet axis where particles are strongly energised at recollimation shocks. At lower frequencies, the decay rate being lower, particles from the cocoon also contribute to the emission map, resulting in a nearly homogeneous volume filling cocoon.

4. Publications

The results have been obtained thanks to the time allocation through the INAF-CINECA MoU. The simulations are very computationally demanding, due to the hybrid particle-fluid schemes. However, thanks to the available resources, we are for the first time able to explore realistic simulations of relativistic jets, which have better conformity with observed results, than any previous work. The results from this project is expected to yield several publications, of which the first has been published, and the rest are in preparation, as listed below:

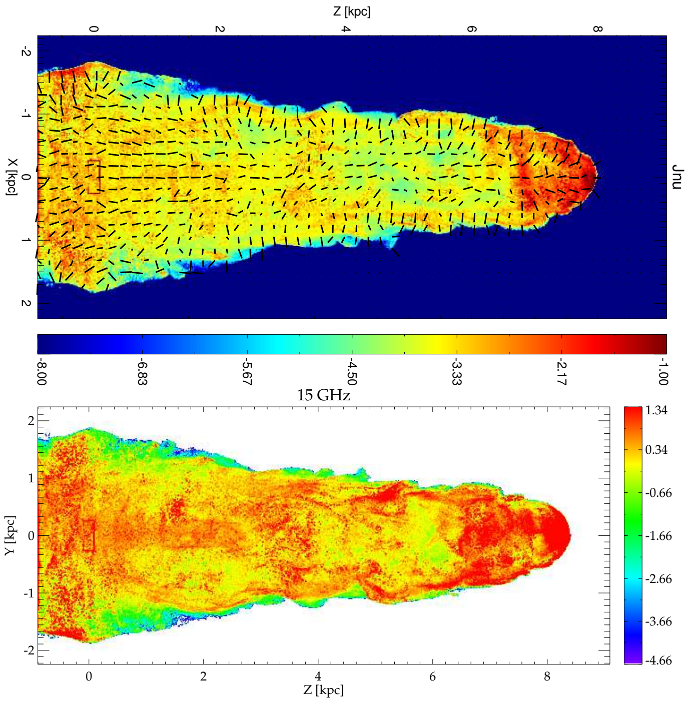

Fig. 2. Top: Morphology of synchrotron emission at 1.4 GHz for simulation G , in normalised units of surface brightness. The black vectors represent the direction of electric field projected on the plane of observation, showing the polarisation of the emission. The length of the vectors are adjusted to represent the fractional polarisation. **Bottom:** The synchrotron surface brightness at 15 GHz.

– D. Mukherjee, G. Bodo, A. Mignone, P. Rossi & B. Vaidya, *Simulating the dynamics and non-thermal emission of relativistic magnetised jets I. Dynamics*, 2020, MNRAS, submitted
– D. Mukherjee, G. Bodo, A. Mignone, P. Rossi & B. Vaidya, *Simulating the dynamics and synchrotron emission from relativistic jets II. Emission at radio bands*, 2020, in preparation
– D. Mukherjee, G. Bodo, A. Mignone, P. Rossi & B. Vaidya, *Simulating the dynamics and synchrotron emission from relativistic jets III. High energy emission from jets*, 2020, in preparation

Acknowledgements. We acknowledge the computing centre of Cineca and INAF, under the coordination of the "Accordo Quadro MoU per lo svolgimento di attività congiunta di ricerca Nuove frontiere in Astrofisica: HPC e Data Exploration di nuova generazione", for the availability of computing resources and support.

References

Colella, P., and Woodward, P. R. 1984, J. Comput. Phys., 54, 174
Fabian, A. C. 2012, ARA&A, 50, 455
Fanaroff, B. L., and Riley, J. M. 1974, MNRAS, 167, 31P
Jaffe, W. J., and Perola, G. C. 1973, A&A, 26, 423
Mignone, A., et al. 2007, ApJS, 170, 228
Mignone, A., Ugliano, M., and Bodo, G. 2009, MNRAS, 393, 1141
Mimica, P., and Aloy, M. A. 2012, MNRAS, 421, 2635
Mimica, P., et al. 2004, A&A, 418, 947
Mukherjee, D., et al. 2020, MNRAS, 499, 681
Murgia, M., et al. 1999, A&A, 345, 769

Pacholczyk, A. G. 1970, Radio astrophysics. Nonthermal processes in galactic and extragalactic sources (W. H. Freeman, San Francisco)
Turner, R. J., and Shabala, S. S. 2015, ApJ, 806, 59
Vaidya, B., et al. 2018, ApJ, 865, 144
Worrall, D. M., and Birkinshaw, M. 2006, Multiwavelength Evidence of the Physical Processes in Radio Jets, in Physics of Active Galacic Nuclei at all Scales, ed. D. Alloin et al. (Springer, Berlin), LNP, 693, 39